



Evaluation of the effect of local rotation and vertical displacements modes in the nonlinear seismic response of steel frames

Federico Valenzuela-Beltran^a, Mario D. Llanes-Tizoc^a, Eden Bojorquez^b, Juan Bojorquez^a, Alfredo Reyes-Salazar^{b,*}

^a Facultad de Ingeniería, Universidad Autónoma de Sinaloa, Ciudad Universitaria, Culiacán, Sinaloa CP 80000, Mexico

^b Facultad de Ingeniería, Universidad Autónoma de Sinaloa, Ciudad Universitaria, Culiacán, Sinaloa CP 80000, Mexico

ARTICLE INFO

Keywords:

Nonlinear seismic response
Steel frames
Rayleigh damping
Superposition of modal damping matrices
Higher mode effects
Effective modal mass

ABSTRACT

Seismic analysis of buildings is normally based on a damping matrix derived from the Rayleigh Model (C_R). However, it is accepted that the damping matrix (C_S) derived from the superposition of modal damping matrices (SMDM) gives more accurate results. Another issue related to seismic analysis of structures consists in the overlooking of the contribution of the modes associated to local rotations (LR) and vertical displacements (VD). The main purposes of this paper are to illustrate the inconvenience of using the C_R matrix and to evaluate the contribution of the LR and VD modes. To this aim, the nonlinear seismic responses of three steel building models idealized as complex 2D MDOF systems under the action of several seismic records are calculated. The major finding of the paper are: (a) The underestimation of axial loads and bending moments can be larger than 40% and 30%, respectively, if the matrix C_R is used; (b) if only lateral displacements (LD) modes are used to generate C_S , some damping should be given in LR and VD modes to avoid amplification of the response; (c) the combined contribution of the LR and VD modes to axial loads, bending moment can be, on an average basis, larger than 50% and 17%, respectively, while for interstory shears and drifts it can be larger than 20%. In light of the findings of this study, it is strongly recommended to use the SMDM procedure to form the damping matrix and to consider the contributions of the LR and VD modes when calculating the seismic response. The presented study was limited to plane frames that are regular in-plan and elevation. Other aspects like irregularity and 3D models need to be considered to get more general conclusions.

1. Introduction

While analyzing seismically a concrete or steel structure, it is common to use the Rayleigh damping matrix (C_R), which is calculated via a combination of the mass (M) and stiffness matrices (K) through the use of the proportional coefficients named α and β [1–3].

This damping model is broadly used in seismic analysis of steel buildings and is included in most of the software developed for this purpose. It is important to mention that energy dissipation produced by hysteretic behavior of the material is not included in C_R , but it is considered through the nonlinear constitutive relation between forces and deformations (hysteretic force–deformation relationship) of the structural members. Such a viscous damping matrix should be viewed as an equivalent viscous damping model since, except for the dissipation of energy associated to yielding of the structural members most of the sources of energy dissipation are supposed to be considered. Such

sources include: (a) thermal effects produced by repeated elastic deformation of structural materials, (b) friction between the boundaries of such material grains, (c) repeated deformations of nonstructural elements, such as partition walls, fireproofing and mechanical equipment, (d) friction between the main structural members and nonstructural members, (e) friction occurring in connections of steel structures and (f) friction due to opening and closing of micro-cracks in the case of concrete members.

The construction of the C_R matrix is consistent with values of modal damping ratios (ζ) which are obtained from system identification methods applied to structural motions produced by earthquakes. However, only two damping modal ratios (ζ_i and ζ_j) can be used in the Rayleigh damping model. In traditional textbooks about structural dynamics [1–3], it is stated that if the two modes used to calculate the coefficients of the C_R matrix are properly selected, all the modes that contribute significantly to the response will be considered and the

* Corresponding author.

E-mail address: reyes@uas.edu.mx (A. Reyes-Salazar).

<https://doi.org/10.1016/j.engstruct.2023.116097>

Received 7 March 2022; Received in revised form 22 March 2023; Accepted 2 April 2023

Available online 15 April 2023

0141-0296/© 2023 Elsevier Ltd. All rights reserved.

responses of very high-frequency modes will be effectively eliminated due to the large values of damping in such modes. The authors believe that these statements are for the case of elastic behavior and for modes associated to lateral vibration. Nothing is said, however, regarding the influence of inelastic behavior and the effects of modes associated to local joint rotation (LR) or to vertical displacements (VD), which may contribute significantly to the seismic response, particularly in terms of local parameters as axial loads on columns.

Many problems arise from the use of the Rayleigh damping model that deserve our attention:

- (a) The use of the Rayleigh damping model will automatically lead to damping ratios in the superior modes much larger than those of the i and j modes which in turn may produce unrealistic very large damping forces.
- (b) Experimental data indicate that the magnitude of ζ_n is roughly the same for several modes, which contradicts what is adopted in the Rayleigh model.
- (c) If the elastic stiffness matrix (\mathbf{K}_0) is used in \mathbf{C}_R , the elements (C_{Rij}) of such a matrix will not tend to decrease as the structure reduces its stiffness due to inelastic behavior and so the modal damping ratios (C_n). Since the magnitude of the vibration frequencies (ω_n) reduces after yielding, the damping ratio for any mode ($\zeta_n = C_n/(2M_n\omega_n)$) will increase leading to inaccuracies in the results.
- (d) The abovementioned increments in the ζ_n values are partially compensated by using the tangent stiffness matrix K_t instead of K_0 ; in this sense, K_t represents a better option than K_0 .
- (e) The dissipated energy produced by thermal effects of repeated elastic deformations and from the friction among the boundaries of the grains within elastic behavior also occurs after the material yields. Again, in this sense, using K_t is more reasonable than K_0 since the magnitude of the C_{Rij} elements is expected to reduce due to the degradation of structural stiffness produced by inelastic behavior.
- (f) However, if \mathbf{C}_R is derived from K_t , damping will experiment hysteretic behavior as the structure does, implying that when the velocity of the structure goes to zero after the ground stops shaking, the damping forces will not go to zero, but there will be a certain value due to residual plastic deformations in the structural members.

From the above discussion it is clear that the use of the Rayleigh damping model leads to some problems, even if the K_t matrix is used. In this regard, it is more convenient to use a damping matrix (\mathbf{C}_S) derived from the superposition of modal damping matrices (SMDM) [4]. However, nothing has been stated regarding the contribution of the higher modes of vibration. As will be further described below, illustrating a few of the inconveniences of using the \mathbf{C}_R damping matrix is one of the objectives of this paper. In addition, the contribution of LR and VD modes, participating in the damping matrix, in terms of common used response parameters, including global and local, is also studied.

2. Literature review

Many investigations have been conducted concerning the damping matrix formulation. Among the first works we can find that of Rea et al. [5], where the damping capacity of steel frames was evaluated by using a steel platform supported on columns. Because it was a strong-beam-weak-column system the inelastic deformations were concentrated on the columns and the ductility capacity was only slightly greater than unity. Wilson and Penzien [6] by using simplified systems proposed two procedures to numerically evaluate the damping matrix. The seismic responses of reinforced concrete structures were studied by Crips [7] considering several damping models, but only 6- and 12-story models were considered. Léger and Dussault [8] using simplified MDOF systems, analyzed the inconveniences of using viscous damping to

represent dissipated energy in structures modeled as complex systems. Bernal [9] showed, for inelastic response of structures with initial orthogonality, that in systems with massless coordinates, the loss of orthogonality can lead to spurious damping forces. The differences between the nonlinear seismic responses of buildings with viscous and hysteretic damping, idealized as SDOF systems, were addressed by Val and Segal [10]. Hall [11] considering shear buildings found that the damping forces generated by the Rayleigh damping matrix obtained from using the initial linear stiffness matrix are unrealistically large resulting in unconservative designs. Li and Wu [12] developed relationships between ductility and damping to be used with the direct DB-SD method. To minimize inaccuracies resulting from the use of the Rayleigh damping matrix in structures deforming into the inelastic range, Zareian and Medina [13] proposed modeling each structural element as elastic with stiffness-proportional damping, and two springs at the ends with no stiffness-proportional damping. Rodrigues et al. [14] based on the experimental results of single columns, developed a model to calculate equivalent viscous damping in reinforced concrete columns. Jehel et al. [15] contrasted the results of the initial stiffness with those of the tangent stiffness, for the case of the Rayleigh model. Carr et al. [16] after studying the inconveniences derived from the use of the Rayleigh damping model, suggested a simplified model for viscous damping; only one 4-story building and displacement as a response parameter were considered. Kollar and Pap [17] extended the Foppl's Approximation to calculate the modal mass, natural frequency and damping ratio and applied it to the vibration of floors supported by beams.

Some other studies have focused on the evaluation of procedures and improving the state of the art regarding the design of steel buildings [18,19]. Ferraioli et al. [20] conducted a study to examine the impact of crucial parameters in the force-controlled design of steel buildings. Their findings led them to propose a local ductility criterion, which aims to enhance the design procedures outlined in the Italian code for steel building design. Elghazouli [21] analyzed the techniques and procedures used in the seismic design of steel frames, focusing on the provisions in Eurocode 8. The authors emphasize the importance of careful consideration of stability and drift requirements, capacity design checks in moment frames, post-buckling response, and distribution of inelastic demand in braced frames. Landolfo [22] offers a revision of the European standards for the design and verification of structures. The paper summarizes the critical issues in the field of steel structures in seismic areas and the recent and ongoing research activities that justify the normative updates. Although the referred investigations point out the areas for improvement in the design process of steel structures, no discussion is offered regarding some aspects that are very important in their seismic response, such as the model for the damping matrix, as well as the consideration of vibration modes that can play an important role in the seismic behavior of steel buildings. This point is discussed further at the end of this section.

More recently, Zhang et al. [23] by considering a displacement-dependent damping model for structures idealized as SDOF systems estimated the equivalent viscous damping introduced by bolted joints. The responses of moment-resisting and concentrically-braced steel frames for several viscous damping models were studied by Zand and Akbari [24]. Milanchian and Hosseini [25] based on the response of SDOF models with nonlinear viscous dampers proposed a procedure to evaluate the response of SDOF systems with linear viscous dampers. Jafari and Alipour [26] found that conventional dampers used to reduce vibrations of structures subjected to wind loads need to be further studied. Qian et al. [27] showed that linear damping models are adequate to estimate seismic demands on steel moment-frame buildings as long as the frames are designed to satisfy current story drift and plastic rotation limits. Sun et al. [28] proposed an adaptive viscous damping wall system that combines a viscous damping wall with lead dampers through working gaps.

Studies regarding the consideration of high modes of vibration in the damping matrix have also been conducted. Clough [29] quantitatively

estimated the influence of the second and third modes of vibration on the seismic response of a tall building. Maniatakis et al. [30] investigated the contribution of higher modes on the global response of a nine-storey moment-resisting RC frame structure. Qiu and Zhu [31] numerically investigated the behavior of multi-story steel frames with self-centering braces (SCBs) by using pushover and incremental seismic analyses. They compared the performance of this system with that of buckling-restrained braced frames emphasizing the high-mode effect. It was shown that the high-mode effect is more significant for high seismic intensities. Vafaei and Alih [32] by using cantilever structures experimentally and analytically studied the effects of higher order modes as well as of different mass configurations on the quality of damage detection through Discrete Wavelet Transform. Chen et al. [33] proposed a design procedure for tall steel braced frames with segmental elastic trussed spines to achieve uniform storey drift response. Such a method combines the forces produced by yielding and the forces produced by higher modes involving the flexural dynamic response of elastic truss segments. Chopra and McKenna [4] demonstrated that if the damping matrix is formed by SMDM, the spurious damping forces resulting from the Rayleigh damping model are eliminated and that if a distributed plasticity model is used, the structural response is independent of the damping model. Only one seismic record, one building model, and displacements as the response parameter, were considered. Almitani et al. [34] studied the frequency response and modal participation factors of perforated multilayer microbeam structures through finite element analysis. To specify the most suitable vibrational mode for a given degree of freedom for base excitation, the participation factor and the corresponding modal effective mass were analyzed. Lu et al. [35] based on experimental and numerical studies proposed a steel tubular friction damper (STFD) for vibration reduction of spatial structures with large spans, where optimal arrangements of STFDs were analyzed based on additional modal damping ratios. Rahmani et al. [36] proposed a nonlinear static analysis procedure to assess the seismic performance of tall buildings, considering the higher modes effects and the progressive changes in the dynamic properties of the building due to nonlinear response. Kinoshita et al. [37] conducted an investigation oriented at estimating the first-modal natural periods and damping ratios of buildings in the vertical direction and proposed an equation to calculate the first-mode vertical natural period. Bhattacharjee et al. [38] developed seismic design guidelines for asymmetric single and multi-story structures supported on combined piled raft foundations considering torsional and higher modes effects. Gremer et al. [39] performed time-history nonlinear analyses to predict horizontal and vertical acceleration responses in steel moment frames using modified versions of Rayleigh damping and the modal damping. The main results indicate that modal damping modelling or modified versions of Rayleigh damping should be considered to have reasonable predictions of both horizontal and vertical frame acceleration demands. Luco and Lanzani [40] presented a detailed study to investigate the inelastic seismic response of simple multilevel frames with massless degrees of freedom for three damping models. They found that some nonzero damping forces/moments at massless DOFs obtained for the case of Rayleigh damping with tangent stiffness may be numerical artifacts rather than a deficiency of the damping model. In another study Luco and Lanzani [41] proposed a new damping model in which the inherent damping forces are considered to be in terms of the restoring forces. The proposed damping model was found to be computationally efficient for the analysis of a 10-degree of freedom building model. Cruz and Miranda [42] examined damping ratio in tall buildings. They found that the damping ratio values decrease with the height of the models. Bernal et al. [43] developed simple expressions to calculate the first-mode damping ratio through regression analyses. It was found that the effective damping ratio is greater than 2 % for steel buildings and very close to 5 % for reinforced concrete buildings.

Many studies have been conducted to evaluate the accuracy of using specific damping models and the contribution of higher modes of

vibration in the estimation of the structural response. However, many issues need to be additionally studied. A comparison of the responses obtained from the Rayleigh damping model with those of a more accurate damping model, as that resulting from the SMDM procedure, for low-, mid- and high-rise steel frames idealized as complex (MDOF) systems, considering several response parameters at both local and global levels, has not been performed. Similarly, studies evaluating the contribution of the higher frequency joint rotation modes, or those modes associated to vertical displacements, considering complex models, have not been conducted either. Some of these issues are addressed in this investigation.

3. Objectives

The specific objectives of this research are:

Objective 1. To calculate the natural frequencies and modal shapes of vibration including those associated to LR and VD modes for the models under consideration; the order of the modes will be particularly discussed. In order to illustrate the need for damping in the LR and/or VD modes, the seismic responses are calculated by using the C_S damping matrix considering $\zeta = 0\%$ in such modes.

Objective 2. In order to illustrate the inaccuracies of the Rayleigh damping model, the results obtained from this model, in terms of many response parameters, are compared with those obtained from the SMDM.

Objective 3. To calculate the simultaneous contribution of the LR and VD modes.

Objective 4. To separately calculate the contribution of the LR and VD modes.

4. Procedure and models used in the study

Three steel building models represented by plane frames, which in turn are idealized as MDOF systems, and twenty seismic records are considered in this study. The Ruaumoko Computer Program [44] is used to calculate the nonlinear seismic responses in terms of several parameters. The Newmark average acceleration method is used to solve the equilibrium differential equation system where an integration time step (Δt) of 0.001 s is adopted. The second-order effects are taken into account in the analyses. The vertical structural members are modeled by a single element as beam-columns while the horizontal ones as beams, which in turn are divided into two elements by defining a node at the mid-span in such a way that for the case of the 3-story model, 25 nodes are considered including the four fixed supports. Three degrees of freedom per node are used. Under these considerations and taking into account the support conditions, the total number of DOFs is 63 and 319 for the 3-story and 9-story models, respectively. The corresponding numbers for the 20-story building are 698 and 825 for the NS and EW directions, respectively.

In addition to the earlier considerations, the concentrated mass model is adopted in the analysis where zero inertia was assigned to the rotational DOFs, the panel zone is assumed to be rigid and the hysteretic behavior of the members is taken as bilinear with 3 % of post-elastic stiffness. The concentrated plasticity approach is used and the interaction between axial loads and bending moments is defined according to the model proposed by Chen and Atsuta [45]. Additional information particularly for the structural models and the seismic records is given in the following sub-sections.

4.1. Structural models and seismic records

SAC commissioned three consulting firms to perform code designs for 3-, 9-, and 20-story model buildings, according to the code requirements of three cities (Los Angeles, Seattle and Boston) [46]. The prevailing requirements for gravity, wind, and seismic design were

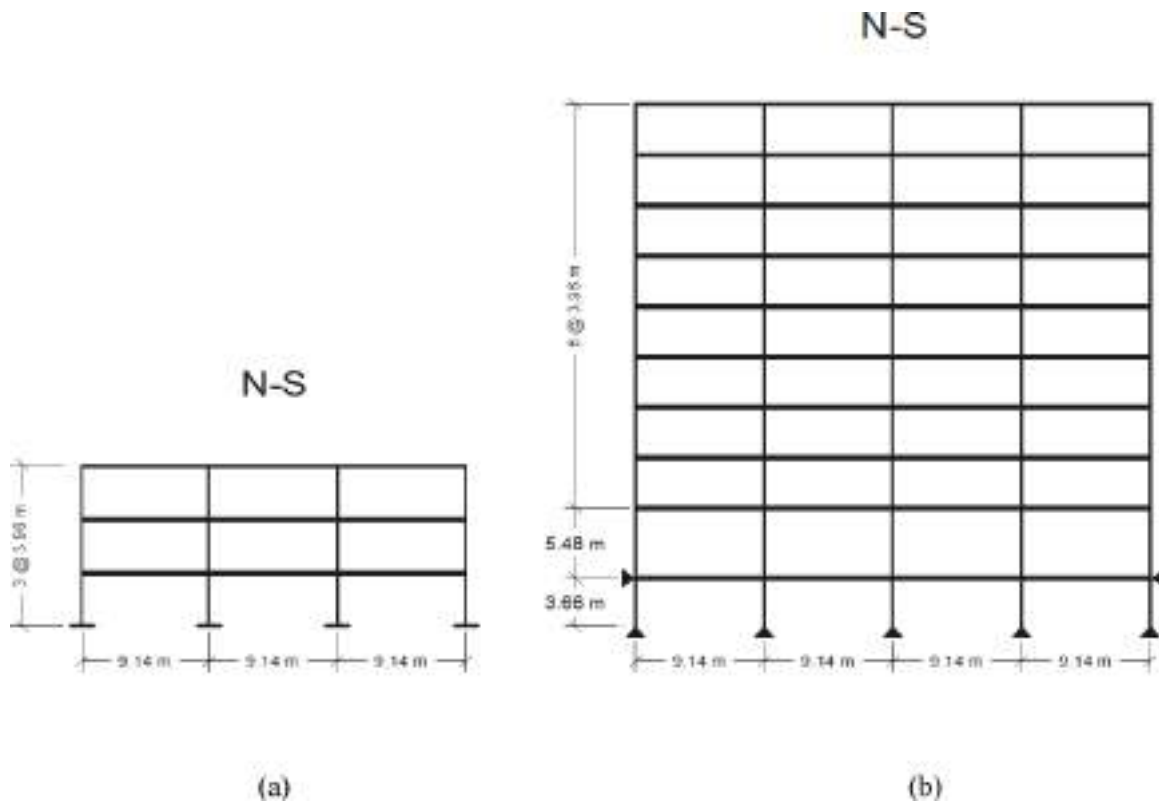


Fig. 1. Model elevations; (a) 3-storey model, (b) 9-story.

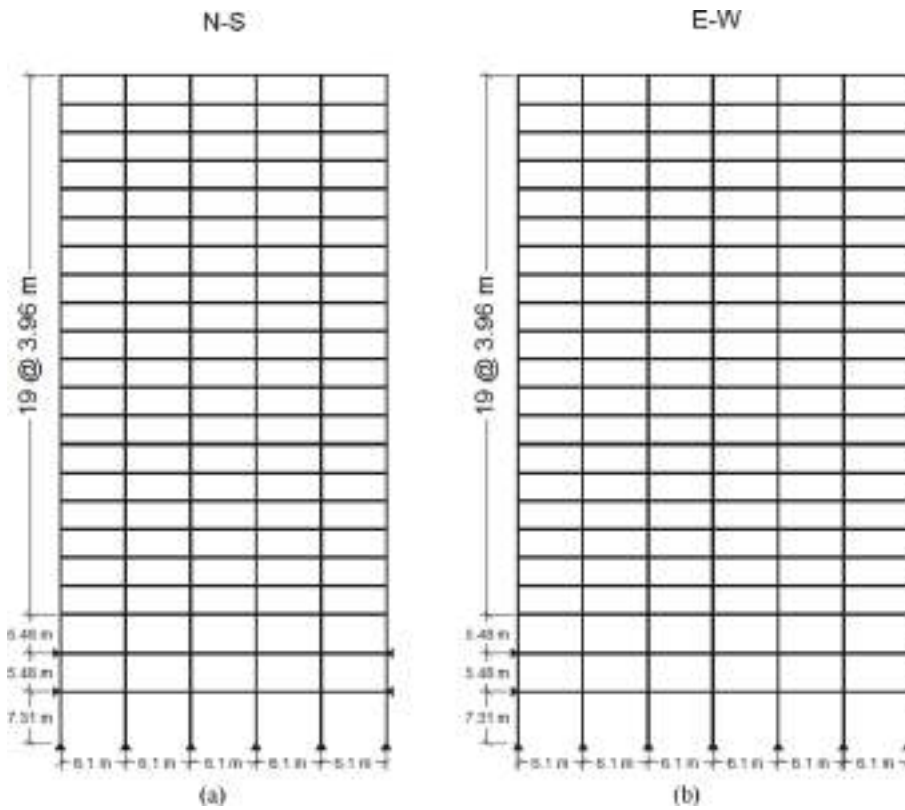


Fig. 2. Elevation of the 20-storey model, (a) NS direction, (b) EW direction.

Table 1
Beam and column sections, Models 1 and 2.

| Model | Story | Columns | | Girders |
|---------|------------|-----------|-----------|-----------|
| | | Exterior | Interior | |
| 3-Level | 1 | W14 × 257 | W14 × 311 | W33 × 118 |
| | 2 | W14 × 257 | W14 × 311 | W30 × 116 |
| | 3/Roof | W14 × 257 | W14 × 311 | W24 × 68 |
| 9-Level | Basement-1 | W14 × 370 | W14 × 500 | W36 × 160 |
| | 1 | W14 × 370 | W14 × 500 | W36 × 160 |
| | 2 | W14 × 370 | W14 × 500 | W36 × 160 |
| | 3 | W14 × 370 | W14 × 455 | W36 × 135 |
| | 4 | W14 × 370 | W14 × 455 | W36 × 135 |
| | 5 | W14 × 283 | W14 × 370 | W36 × 135 |
| | 6 | W14 × 283 | W14 × 370 | W36 × 135 |
| | 7 | W14 × 257 | W14 × 283 | W30 × 99 |
| | 8 | W14 × 257 | W14 × 283 | W27 × 84 |
| 9/roof | W14 × 233 | W14 × 257 | W24 × 68 | |

Table 2
Beam and column sections Model 3.

| Story | Columns | | Girders |
|------------|----------------|-----------|-----------|
| | Exterior | Interior | |
| Basement-1 | 15 × 15 × 2.0 | W24 × 335 | W14 × 22 |
| Basement-2 | 15 × 15 × 2.0 | W24 × 335 | W30 × 99 |
| 1 | 15 × 15 × 2.0 | W24 × 335 | W30 × 99 |
| 2 | 15 × 15 × 2.0 | W24 × 335 | W30 × 99 |
| 3 | 15 × 15 × 1.25 | W24 × 335 | W30 × 99 |
| 4 | 15 × 15 × 1.25 | W24 × 335 | W30 × 99 |
| 5 | 15 × 15 × 1.25 | W24 × 335 | W30 × 108 |
| 6 | 15 × 15 × 1.0 | W24 × 229 | W30 × 108 |
| 7 | 15 × 15 × 1.0 | W24 × 229 | W30 × 108 |
| 8 | 15 × 15 × 1.0 | W24 × 229 | W30 × 108 |
| 9 | 15 × 15 × 1.0 | W24 × 229 | W30 × 108 |
| 10 | 15 × 15 × 1.0 | W24 × 229 | W30 × 108 |
| 11 | 15 × 15 × 1.0 | W24 × 229 | W30 × 99 |
| 12 | 15 × 15 × 1.0 | W24 × 192 | W30 × 99 |
| 13 | 15 × 15 × 1.0 | W24 × 192 | W30 × 99 |
| 14 | 15 × 15 × 1.0 | W24 × 192 | W30 × 99 |
| 15 | 15 × 15 × 0.75 | W24 × 131 | W30 × 99 |
| 16 | 15 × 15 × 0.75 | W24 × 131 | W30 × 99 |
| 17 | 15 × 15 × 0.75 | W24 × 131 | W27 × 84 |
| 18 | 15 × 15 × 0.75 | W24 × 117 | W27 × 84 |
| 19 | 15 × 15 × 0.75 | W24 × 117 | W24 × 62 |
| 20/Roof | 15 × 15 × 0.5 | W24 × 84 | W21 × 50 |

Table 3
Strong motion.

| Seismic Record | Earthquake name | Sation | M _w | ED (km) | PGA (g) | | T (s) | |
|----------------|--------------------------|----------------------|----------------|---------|---------|------|-------|------|
| | | | | | N-S | E-O | N-S | E-O |
| 1 | Northridge 01 | Sun Valley | 6.7 | 5.6 | 0.45 | 0.28 | 0.18 | 0.20 |
| 2 | Northridge 01 | Beverly Hills | 6.7 | 9.4 | 0.49 | 0.44 | 0.53 | 0.52 |
| 3 | Northridge 01 | LA - W 15th St | 6.7 | 25.6 | 0.17 | 0.10 | 0.36 | 0.38 |
| 4 | Northridge 01 | LA - Baldwin Hills | 6.7 | 23.5 | 0.17 | 0.24 | 0.17 | 0.28 |
| 5 | El Mayor Cucapah, Mexico | El Centro - MUS | 7.2 | 27.8 | 0.20 | 0.19 | 0.44 | 0.23 |
| 6 | El Mayor Cucapah, Mexico | El Centro - MGA | 7.2 | 28.5 | 0.29 | 0.44 | 0.12 | 0.15 |
| 7 | Landers | Coolwater | 7.3 | 19.7 | 0.42 | 0.28 | 0.36 | 0.33 |
| 8 | Landers | North Palm Springs | 7.3 | 26.8 | 0.13 | 0.14 | 0.18 | 0.20 |
| 9 | Landers | Mission Creek Fault | 7.3 | 27.0 | 0.13 | 0.13 | 0.29 | 0.17 |
| 10 | Landers | Desert Hot Springs | 7.3 | 21.8 | 0.15 | 0.17 | 0.87 | 0.97 |
| 11 | Loma Prieta | Hollister | 6.9 | 27.7 | 0.18 | 0.37 | 0.55 | 0.51 |
| 12 | Loma Prieta | Coyote Lake Dam | 6.9 | 20.4 | 0.16 | 0.18 | 0.19 | 0.20 |
| 13 | San Fernando | LA - Hollywood | 6.6 | 22.8 | 0.19 | 0.22 | 0.12 | 0.10 |
| 14 | Chalfant Valley 02 | Bishop - LADWP | 6.2 | 14.4 | 0.25 | 0.18 | 0.37 | 0.19 |
| 15 | Coalinga 01 | Parkfield | 6.4 | 28.6 | 0.12 | 0.13 | 0.26 | 0.23 |
| 16 | Coalinga 01 | Cantua Creek School | 6.4 | 23.8 | 0.29 | 0.23 | 0.60 | 0.22 |
| 17 | Imperial Valley 06 | Parachute Test Site | 6.5 | 12.7 | 0.21 | 0.11 | 0.13 | 0.21 |
| 18 | Parkfield 02 CA | Coalinga - FS 39 | 6.0 | 22.5 | 0.04 | 0.08 | 0.20 | 0.49 |
| 19 | Cape Mendocino | Fortuna Fire Station | 7.0 | 16.5 | 0.28 | 0.33 | 0.41 | 0.49 |
| 20 | Joshua Tree CA | Thousand Palms PO | 6.1 | 17.2 | 0.20 | 0.20 | 0.15 | 0.27 |

considered. The structural models corresponding to Los Angeles Area for the Post-Northridge recommendations are used in this study to address the issues mentioned in the objectives. The plane models used in this research consist of the perimeter moment frames of the aforementioned 3D buildings. They will be referred hereafter as Models 1, 2 and 3, respectively. The elevations of the 3- and 9-level models are presented in Fig. 1 while that of the 20-level is given in Fig. 2. The sections of the structural members can be seen in Tables 1 and 2. There are no column splices in the 3-story model, but in the 9- and 20-story models splices are located in every-two and three stories, respectively. Additional information about these models can be found in the literature [46].

To take into account the seismic hazard of the zone, the models are excited by 20 seismic records representative of the model site location. Such records were obtained from the National Strong Motion Project of the United States Geological Survey and were selected so, on an average basis, their spectral values matched that of the 5 %-damped Maximum Considered Earthquake response spectrum associated to the site within the range of 0.2 to 2.0 times the fundamental period of the structural model. In addition, the seismic records belong to seismic events within the same general tectonic regime and have magnitudes and fault distances as those controlling the target spectrum. Table 3 summarizes the main characteristics of the ground motions.

The structural models are simultaneously subjected to the action of both the vertical and the horizontal components of the seismic records; the gravity loads are also considered. The seismic records are scaled to produce different levels of deformation including significant inelastic behavior. This is made according to the geometric mean of spectral acceleration (S_{avg}) [47,48] which is calculated as the “average” of the pseudo-accelerations (S_a) over a range of periods. The range of periods to calculate (S_{avg}) goes from $0.2 T_1$ to $1.6 T_1$ with constant increments of $0.01 s$, where T_1 is the fundamental period of the model. The values of S_{avg} range from $0.2g$ up to $1.4g$ with uniform increments of $0.2g$ for the 3-level building, while for the 9-level model such a range goes from $0.1g$ up to $0.8g$ with constant increments of $0.1g$. For the case of the 20-story model, the range of variation of S_{avg} goes from $0.05g$ to $0.35g$ with constant increments of $0.05g$. It is important to clarify that the maximum values of S_{avg} were chosen in such a way that a similar magnitude of the maximum inelastic deformation were developed in the three models (maximum drift of about 3.5 %).

Table 4
Modal frequencies and type of modes for the 3-level Model.

| MODE | T(s) | EMM (%) | TYPE | MODE | T(s) | EMM (%) | TYPE | MODE | T(s) | EMM (%) | TYPE |
|------|-------|---------|-------|------|-------|---------|------|------|-------|---------|------|
| 1 | 1.073 | 83–42 | LD-LR | 7 | 0.100 | 48 | LR | 13 | 0.069 | 0 | NA |
| 2 | 0.350 | 13 | LD | 8 | 0.099 | 48 | VD | 14 | 0.065 | 0 | NA |
| 3 | 0.189 | 3 | LD | 9 | 0.094 | 0 | NA | 15 | 0.053 | 0 | NA |
| 4 | 0.169 | 0 | NA | 10 | 0.091 | 43 | VD | 16 | 0.051 | 0 | NA |
| 5 | 0.124 | 0 | NA | 11 | 0.091 | 5 | LR | 17 | 0.036 | 4 | VD |
| 6 | 0.108 | 0 | NA | 12 | 0.072 | 0 | NA | 18 | 0.033 | 4 | LR |

NA = NO APPLICABLE.

4.2. Damping models

Since the Rayleigh damping model is broadly used in seismic analysis of steel buildings and is widely cited in the literature [1–3], only the damping matrix (C_S) obtained from the SMDM is briefly described here. In this procedure, it is possible to assign a certain percent of viscous damping in any number of modes, while developing the damping matrix.

The transformation of the damping matrix C_S from geometric to generalized coordinates is given by Eq. (1), where C^N is a diagonal matrix with the n th diagonal element representing the generalized modal damping for the n th mode and can be expressed by Eq. (2).

$$C^N = \phi^T C_S \phi \tag{1}$$

$$C_n = 2\zeta_n M_n^N w_n \tag{2}$$

In Eq. (2), ζ_n , M_n^N and w_n , are the damping ratio, the generalized mass, and frequency, respectively, of the n th mode; the other terms were defined before. Eq. (1) can be rewritten as

$$C_S = (\phi^T)^{-1} C^N \phi^{-1} \tag{3}$$

It can be shown that Eq. (3) can be expressed as

$$C_S = M \phi (M^N)^{-1} C^N (M^N)^{-1} \phi^T M \tag{4}$$

Since M^N and C^N are diagonal matrices, Eq. (4) can be rewritten as

$$C_S = M \left(\sum_{n=1}^m \frac{2\zeta_n w_n}{M_n^N} \phi_n \phi_n^T \right) M \tag{5}$$

The n th term in the summation given in Eq. (5) represents the contribution of the n th mode to the damping matrix C_S (with damping ratio ζ_n). Only the first I modes that are expected to contribute significantly to the response are usually considered in such a summation. Hence, if the $I + 1$ to m modes are not included in Eq. (5) will imply a null contribution of such modes to the C_S matrix.

4.3. Effective modal mass (EMM)

The effective modal mass (EMM) is commonly used to determine the type of mode in a structure. In structural dynamics textbooks, EMM is usually discussed for structures that have masses lumped along a vertical axis. In this case EMM is calculated using Eq. (6), where \mathcal{L}_n and M_n^N are the modal earthquake-excitation factor and the modal mass, respectively, for the n th mode. \mathcal{L}_n in turn is calculated with Eq. (7), where M is

the mass matrix and $\mathbf{1}$ is a vector with each element equal to unity; obviously, such a vector will have as many elements as there are degrees of freedom in the structure.

$$\mathcal{L}_n^2 / M_n^N \tag{6}$$

$$\mathcal{L}_n = \Phi_n^T M \mathbf{1} \tag{7}$$

In this paper, however, since plane frames are used in the structural modeling, three degrees of freedom per node are considered. In such a case an equation derived from an extension of Eq. (7) needs to be used to calculate \mathcal{L}_n ; it has the following form:

$$\mathcal{L}_n = \Phi_n^T M \mathbf{q} \tag{8}$$

In Eq. (8), \mathbf{q} is a coefficient influence vector which are displacements obtained from unit support displacements [1]. Unlike the vector $\mathbf{1}$, \mathbf{q} can have values different than unity. Eq. (8) can be easily extended to consider excitation in the vertical direction. It is important to clarify that Eq. (8) applies only to structures with lumped masses.

5. Objective 1: Natural frequencies and the need for damping in the lower LR and VD modes

In the definition of the natural frequencies and modal shapes of vibration required to form the damping matrix, even in the SMDM procedure, the LR or VD modes are not considered. It is the objective of this part of the paper to calculate and discuss how these modes are located with respect to the lateral (LD) ones as well as to illustrate the need to assign damping in the lower LR and VD modes. The contribution of such modes to the seismic response is addressed in the next sections.

5.1. Natural frequencies

All modal shapes and the associated frequencies of the structural models under consideration were calculated by using the Ruaumoko Software [44]. Similarly, all the modes were used in the numerical models and in the development of the damping matrix according to the SMDM procedure. For example, in the case of the 3-story model, which has 36 DOFs, 36 modes were considered. The periods, effective modal masses (EMM), and the type of mode of the 3-, 9-, and 20-level models can be seen in Tables 4, 5, and 6, respectively. It is worth mentioning that modes with a relatively small value of EMM (0.3 and smaller), particularly LR and VD modes, were observed. Since they do not significantly contribute to the response, they were not included in the

Table 5
Modal frequencies and type of modes for the 9-level Model.

| MODE | T(s) | EMM (%) | TYPE | MODE | T(s) | EMM (%) | TYPE | MODE | T(s) | EMM (%) | TYPE |
|------|-------|---------|-------|------|-------|---------|-------|------|-------|---------|------|
| 1 | 2.450 | 83–49 | LD-LR | 7 | 0.215 | 18–24 | VD-LR | 13 | 0.183 | 0 | NA |
| 2 | 0.921 | 11 | LD | 8 | 0.210 | 4–3 | VD-LR | 14 | 0.178 | 0 | NA |
| 3 | 0.532 | 4 | LD | 9 | 0.199 | 44–12 | VD-LR | 15 | 0.169 | 0 | NA |
| 4 | 0.354 | 1 | LD | 10 | 0.197 | 4–1 | VD-LR | 16 | 0.158 | 0 | NA |
| 5 | 0.261 | 1 | LD | 11 | 0.194 | 1–5 | VD-LR | 17 | 0.146 | 0 | NA |
| 6 | 0.223 | 18 | VD | 12 | 0.187 | 1 | VD | 18 | 0.138 | 0 | NA |

NA = NO APPLICABLE.

Table 6
Modal frequencies and type of modes for 20-level Model, EW direction.

| MODE | T(s) | EMM (%) | TYPE | MODE | T(s) | EMM (%) | TYPE | MODE | T(s) | EMM (%) | TYPE |
|------|-------|---------|-------|------|-------|---------|------|------|-------|---------|-------|
| 1 | 4.181 | 81–80 | LD-LR | 8 | 0.366 | 0 | NA | 15 | 0.191 | 0 | NA |
| 2 | 1.460 | 11 | LD | 9 | 0.310 | 0 | NA | 16 | 0.187 | 0 | NA |
| 3 | 0.849 | 4 | LD | 10 | 0.304 | 0 | NA | 17 | 0.169 | 0 | NA |
| 4 | 0.602 | 2 | LD | 11 | 0.257 | 0 | NA | 18 | 0.151 | 0 | NA |
| 5 | 0.459 | 1 | LD | 12 | 0.253 | 0 | NA | 19 | 0.149 | 11–2 | VD-LR |
| 6 | 0.403 | 82–10 | VD-LR | 13 | 0.219 | 0 | NA | 20 | 0.148 | 1 | VD |
| 7 | 0.374 | 3 | LR | 14 | 0.212 | 0 | NA | 21 | 0.120 | 0 | NA |

NA = NO APPLICABLE.

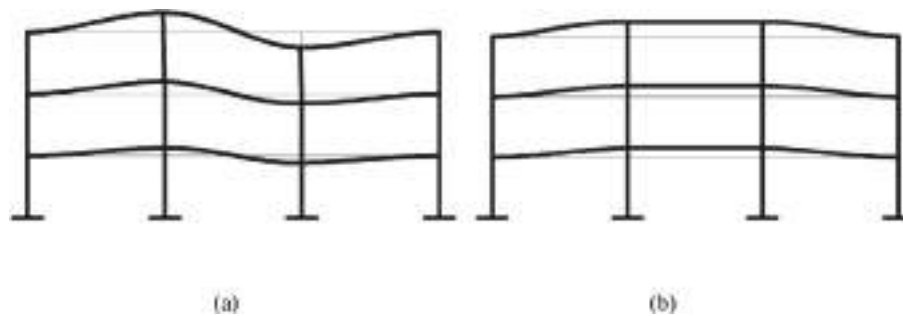


Fig. 3. Some modal shapes for Model 1; (a) Mode 7 (LR), (b) Mode 10 (VD),

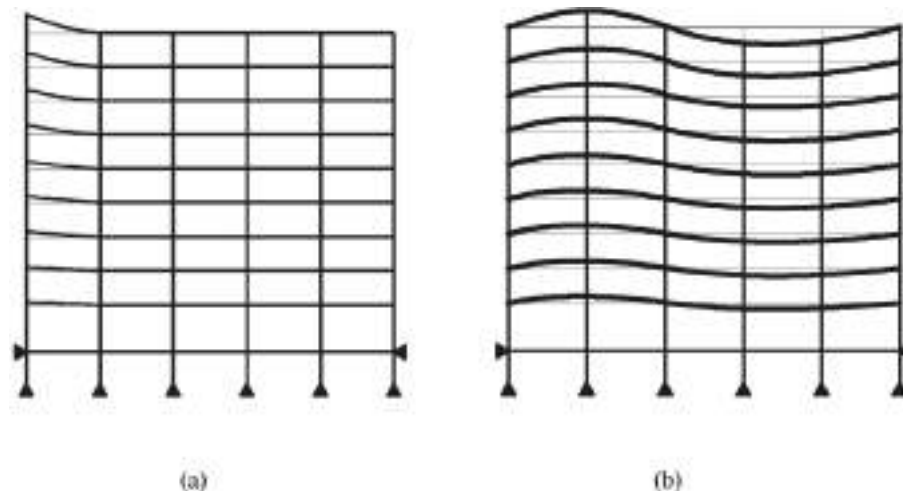


Fig. 4. Some modal shapes for Model 2; (a) Mode 6 (VD), (b) Mode 7 (VD-LR).

tables. Hence, it can be said that the modes that significantly contribute to the response are included in such tables. The concept of EMM is used to determine the type of mode. For a given direction, the EMM of a structure can be interpreted as the part of the total mass responding to an earthquake in each mode [1].

The software used gives the EMM for each mode and each structural direction. In the case of the 3-story model, for example, for Mode 1 the EMMs are 0.83, 0, and 0.42 for displacement in the horizontal direction (LD), vertical direction (VD) and rotations LR, respectively (see Table 4), so this is a combined mode. For Mode 2, on the other hand, the EMMs values are 13, 0, and 0 implying that such a mode is a “pure” LD mode. The corresponding values for Mode 1 of the 9-story building are 0.83, 0, and 0.49. The software also provides a dynamic animation of each mode which helps to identify the type of mode.

As mentioned above, it is not common to include the LR and VD modes in the construction of the damping matrix and even less to calculate their location with respect to the laterals. Seismic analysis software users usually assume that the first “n” periods (n = number of

stories) are associated to LD modes and then those of the LR or VD modes follow. Results of the abovementioned tables indicate that it is not the case for the 9- and 20-level frames; it is clearly shown that the order of the modes may be mixed; for example for the 9-level model the first five modes are LD type, but modes 6 and 7 are VD and LR type, respectively. Just for illustration purposes, a few modal shapes associated to VD and LR modes are given. The modal shapes for Modes 7 and 10 of Model 1 can be seen in Fig. 3a and 3b, respectively, while those for Modes 6 and 7 of Model 2 are shown in Fig. 4a and 4b, respectively.

5.2. The need for damping in the lower LR and VD modes

The responses of the building models are first calculated by developing the damping matrix C_S with $\zeta = 3\%$ in all modes. Then such responses are compared with those obtained by considering $\zeta = 3\%$ in the lateral modes and $\zeta = 0\%$ in the LR and VD modes. The comparison is made in terms of several parameters. However, it is not the objective to make an exhaustive comparison in this case, but only to show that some

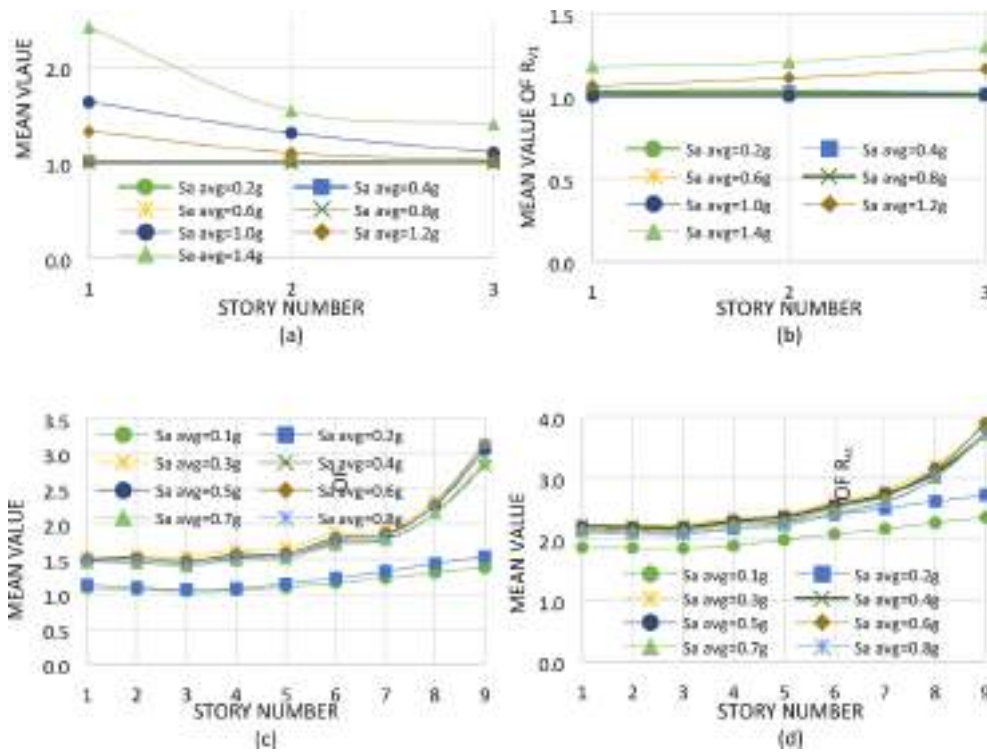


Fig. 5. Effect of using $\zeta = 0\%$ in the LR and VD modes, NS direction; (a) drifts Model 1, (b) shear Model 1, (c) axial load, interior column of Model 2, (d) axial load, exterior column of Model 2.

damping should be given in the LR and VD modes; hence, only a few results are presented.

To make the comparison for interstory displacements, interstory shears and axial loads, the R_{D1} , R_{V1} , and R_{A1} ratios, given by Eqs. (9), (10) and (11), respectively, are used. In Eq. (9) the term D1(3,0) represents the drifts of the models when the damping matrix is formed by considering 3% and 0% in the lateral modes and the LR and VD modes, respectively; the term D1(3,3) represents the same except that 3% of viscous damping were used in all the modes. The numerator and denominator in Eqs. (10) and (11) have a similar meaning but interstory shears and axial loads in columns, respectively, are compared instead. Therefore, a value of one for any of the three above-mentioned ratios will indicate that there is no amplification derived from using $\zeta = 0\%$ in the LR and VD modes; conversely, a value larger than one will indicate that there is some degree of amplification.

$$R_{D1} = \frac{D1(3,0)}{D1(3,3)} \tag{9}$$

$$R_{V1} = \frac{V1(3,0)}{V1(3,3)} \tag{10}$$

$$R_{A1} = \frac{A1(3,0)}{A1(3,3)} \tag{11}$$

The maximum mean values of R_{D1} , R_{V1} and R_{A1} , averaged over all the seismic records used in the study, are shown in Fig. 5 for some cases. Results indicate that for the case of Model 1 there is no amplification of the drifts (Fig. 5a, $R_{D1} \approx 1.0$) if $\zeta = 0\%$ is used in the LR and VD modes for the lowest intensities ($S_{a,avg} = 0.2\text{ g}$ and 0.4 g) of the seismic loading; however, amplifications of up to 140% ($R_{D1} \approx 2.4$) occur for the largest seismic intensity ($S_{a,avg} = 1.4\text{ g}$). It is clearly observed that the amplification decreases as one moves up the frame. The earlier observations made for drifts also apply to the case of interstory shears (Fig. 5b) of Model 1, the only additional observations that can be made are that the magnitude of the amplification is lower (maximum values about 30%)

and that it increases as one moves up the structure.

The amplification of axial loads at interior columns of Model 2 (Fig. 5c) resembles those of drifts in the sense that they are not significant for low intensities of the seismic load and the lower stories (1–6); however, they are considerable for the upper stories (8–9), particularly for the larger seismic intensities; they can be greater than 200% for $S_{a,avg} = 0.2\text{ g}$ and the upper stories. The amplification of axial loads at exterior columns of Model 2 (Fig. 5d) is greater than those of interior columns; they can be up to 270%. Hence the amplification depends not only on the type of response parameter but also on the location of the structural element under consideration. Although only a few results are given, it is worth mentioning that the amplification, in general, tends to increase with the high of the model and with the seismic intensity.

The earlier results show that if the SMDM procedure is used to form the damping matrix, in order to avoid amplification of the response, an amount of damping (namely $\zeta = 3\%$) should be given at least in the lower LR and VD modes.

6. Objective 2: Accuracy of the Rayleigh damping model

Some inconveniences derived from the use of the Rayleigh damping model were described in Section 1 of the paper. In this section, the accuracy of such a model is evaluated by comparing the results obtained from the C_R damping matrix with those of the C_S damping matrix. Despite the comparison was made for many response parameters, only a few results are presented in terms of resultant stresses just to show that significant errors can be introduced into the response if the C_R matrix is used.

To perform the comparison for axial loads and bending moments, the R_{A2} and R_{B2} ratios given by Eqs. (12) and (13), respectively, are used. In Eq. (12) the terms A_R and A_S represent the axial load on columns when the Rayleigh and the SMDM procedures, respectively, are used to develop the damping matrix. B_R and B_S in Eq. (13) have a similar meaning, but bending moments are now being considered.

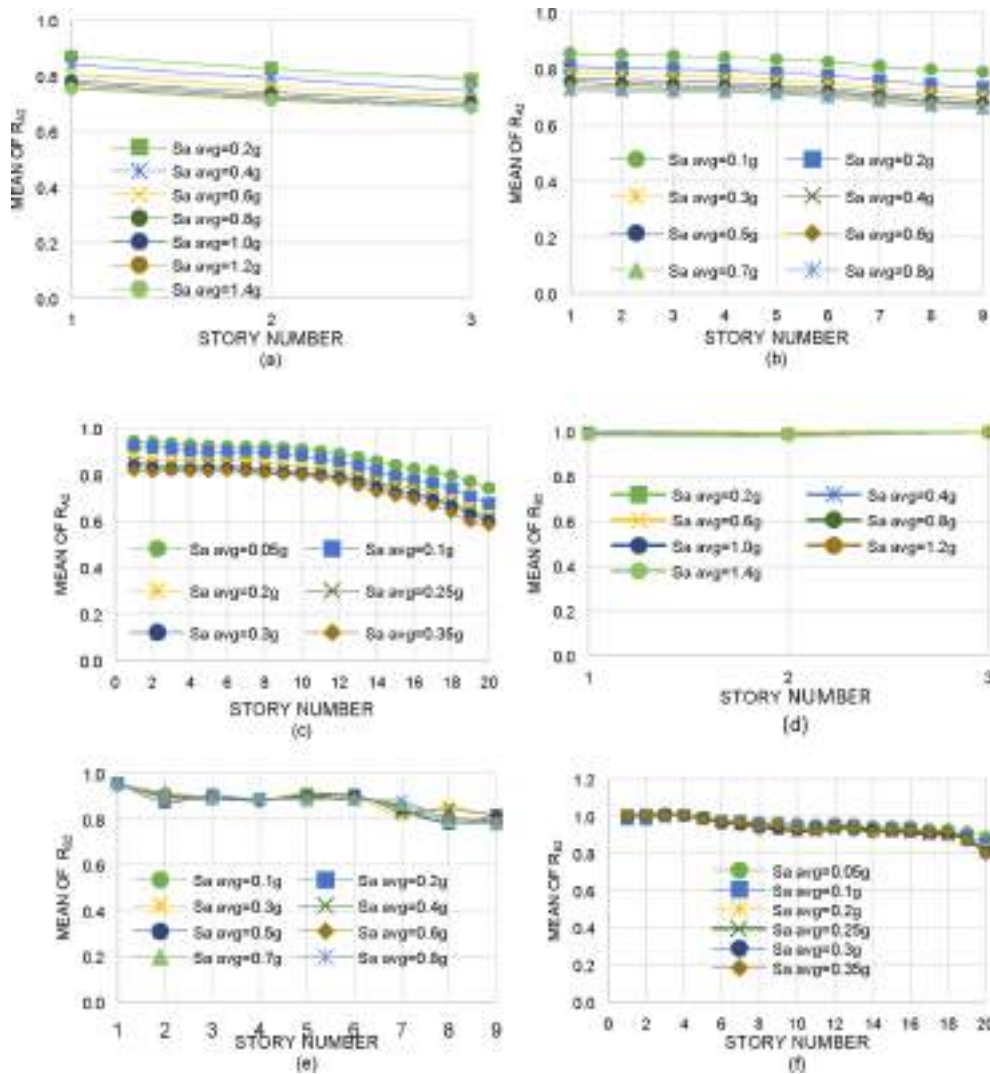


Fig. 6. Average values for R_{A2} and R_{B2} , exterior columns of NS direction: (a), (b) and (c) → R_{A2} for Model 1, 2 and 3; (d), (e) and (f) → R_{B2} Model 1, 2 and 3.

$$R_{A2} = \frac{A_R}{A_S} \tag{12}$$

$$R_{B2} = \frac{B_R}{B_S} \tag{13}$$

The mean values of the R_{A2} and the R_{B2} parameters, averaged over all the seismic records, are shown in Fig. 6. Results indicate that the axial loads on columns may be considerably underestimated if the Rayleigh model is used. The level of underestimation increases as one moves up the model and with the seismic intensity. The maximum values of underestimation increase with the height of the model: they are about 32 %, 35 % and 42 % for the 3-, 9- and 20-storey models, respectively. It is also shown that the underestimation for bending moments, unlike the case of axial loads, is negligible (maximum about 2 %) for the case of Model 1, but underestimations of up to about 22 % and 20 % are observed for Models 2 and 3, respectively. The variation of the magnitude of the underestimation from one seismic intensity to another is much smaller for bending moments than for axial loads. It is worth to mention that, although they are not shown, considerable underestimations also occur for drifts and interstory shears.

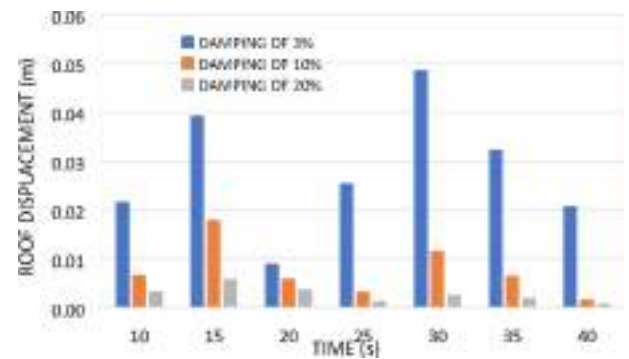


Fig. 7. Top displacements of Model 1, $\zeta = 3\%$, 10 % and 20 %, for first seismic record.

7. Objective 3: Simultaneous contribution of the LR and VD modes

In order to calculate the simultaneous contribution of the LR and VD modes to the seismic response in terms of different parameters, the models under consideration are analyzed by considering $\zeta = 3\%$ of viscous damping in all the modes. Then, the responses are compared

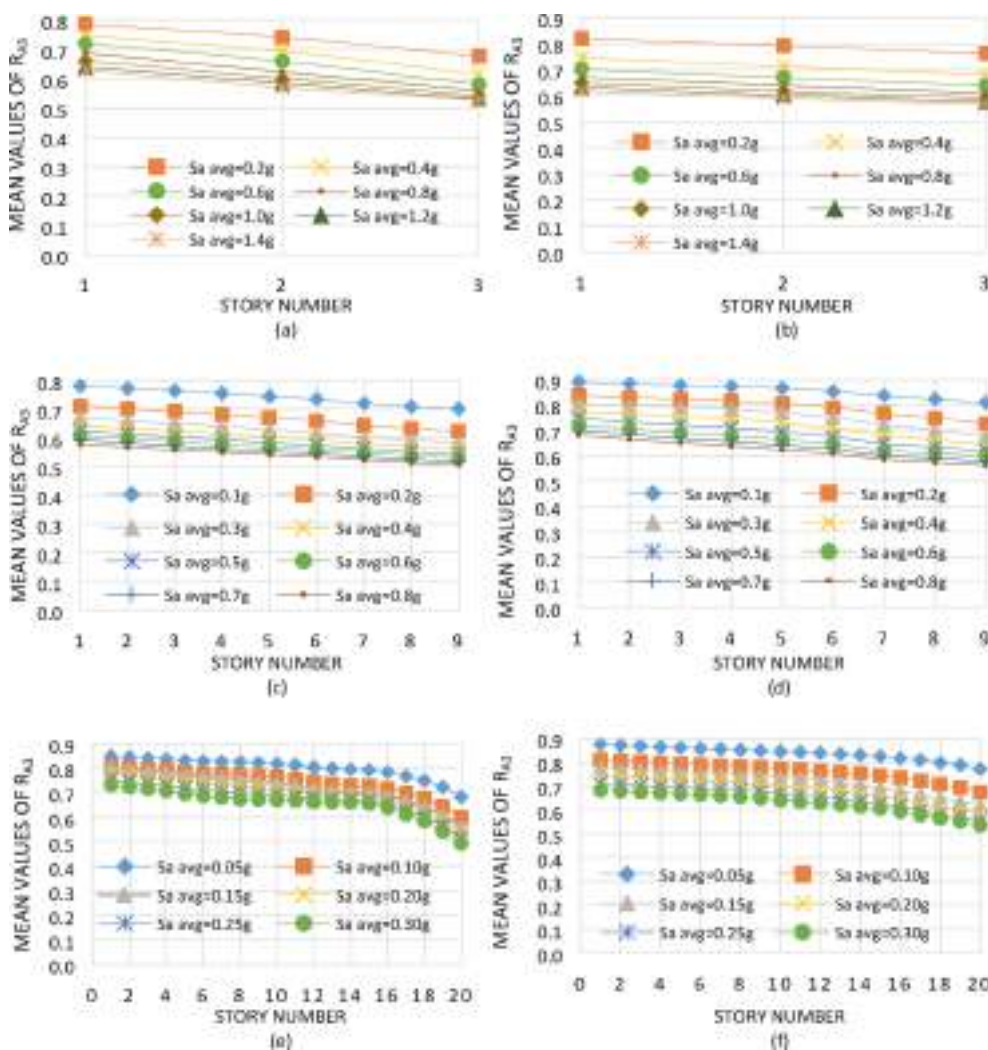


Fig. 8. Contribution of LR and VD modes to axial loads, NS direction; (a) and (b) Ext. and Int. columns, Model 1; (c) and (d) Ext. and Int. columns, Model 2; (e) and (f) Ext. and Int. columns, Model 3.

with those obtained by considering $\zeta = 3\%$ in the lateral modes and $\zeta = 20\%$ in the LR and VD modes. The latter mostly eliminates the participation of the LR and VD modes in the response. Before calculating the contribution of the LR and VD modes, it is shown that considering $\zeta = 20\%$ in all modes practically eliminates the response compared to the response of $\zeta = 3\%$; it is illustrated in Fig. 7 where the top displacement of Model 1 at discrete times under the action of the first seismic record (Table 3) is presented for $\zeta = 3\%$, 10%, and 20% (in all the modes). Since the contribution is not totally eliminated when considering 20% of damping, it is worth mentioning that the actual contributions of such LR and VD modes are larger than those calculated in this paper (Sections 7.1 and 7.2).

7.1. Contributions in terms of local response parameters

To calculate the contribution of the LR and VD modes to axial loads and bending moments on columns, the R_{A3} and R_{B3} quotients given by Eqs. (14) and (15), respectively, are used. In these equations, the first, second, and third numbers in the numerator or the denominator represent the amount of viscous damping assigned in the LD, LR and VD modes, respectively. Thus, in Eq. (14), the term $A3(3,20,20)$ represents the axial load on columns when, to form the damping matrix, 3% of viscous damping is used in the LD modes while 20% is used in the LR and VD modes. The term $A3(3,3,3)$ also represents axial loads except

that 3% of viscous damping is used in all the modes. Therefore, a value of R_{A3} smaller than unity will indicate that there is some contribution of the mentioned modes. The terms in Eq. (15) have a similar meaning to those of Eq. (14), but the contribution for bending moments is now being calculated.

$$R_{A3} = \frac{A3(3, 20, 20)}{A3(3, 3, 3)} \tag{14}$$

$$R_{B3} = \frac{B3(3, 20, 20)}{B3(3, 3, 3)} \tag{15}$$

7.1.1. Axial loads

The mean values of R_{A3} are presented in Fig. 8 for exterior and interior columns of the NS direction for the three models. It is observed that the values can be much less than unity, indicating a significant contribution of the LR and VD modes to the axial loads in columns. For the case of exterior columns of Model 1, the R_{A3} mean values range from 0.79 to 0.53 indicating contributions from 21% to 47%. There is an aspect that the authors would like to emphasize at this state: for the case of Model 1, which has three stories, the first mode is combined (LD-LR) and the second and third ones are LD type. The contribution of the higher modes larger than the third one (LR and VD modes) is evaluated as commented before by assigning 20% of viscous damping in such modes (see Eq. (14)). It is usually believed that the contribution of such

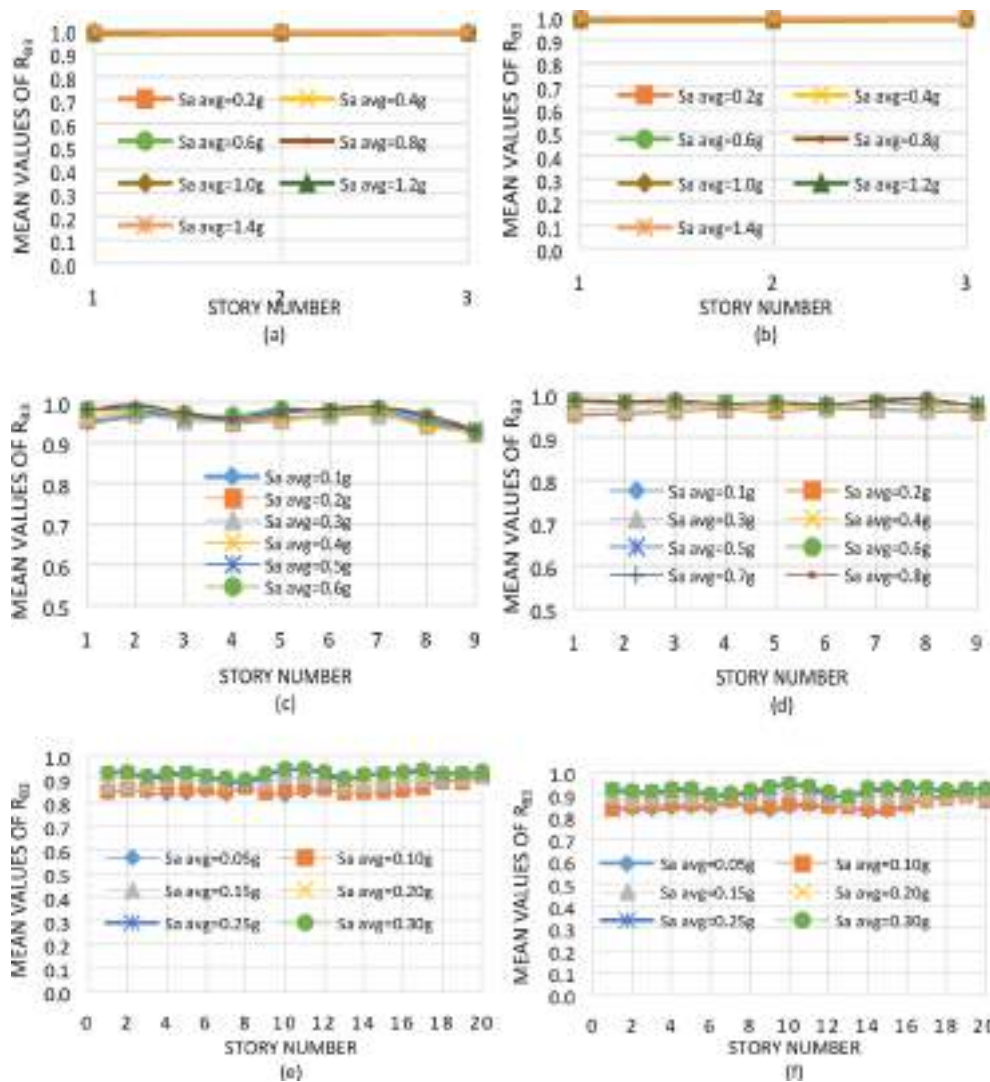


Fig. 9. Contribution of LR and VD modes to bending moments, EW direction; (a) and (b) Ext. and Int. columns, Model 1; (c) and (d) Ext. and Int. columns, Model 2; (e) and (f) Ext. and Int. columns, Model 3.

modes is negligible. The results discussed so far for Model 1, however, indicate that the contribution can be considerable. One of the reasons for this is that the EMM for modes 7 and 8, which are LR and VD modes, is 48 %. In addition, the period of mode 8 (VD) is 0.09 s, which is not so far from 0.07 s, the vertical first mode period of the model.

It is also observed from the results of all models that the contribution tends to increase as one moves up the building and with the seismic intensity. The maximum contribution values are observed to be approximately the same for the three models: they are 47 %, 49 % and 51 % for Models 1, 2 and 3, respectively. Results also indicate that the magnitude of the contribution is slightly smaller for interior columns. The results for the EW direction were also calculated but are not presented; it is worth mentioning, however, that they are quite similar to those of the NS direction.

7.1.2. Bending moments in columns

The mean values of R_{B3} are presented in Fig. 9, in the same order as that of R_{A3} in Fig. 8. The results of the figure indicate that the contribution of the LR and VD modes in terms of bending moments, although smaller than that of axial loads, may be considerable. For Model 1 the contribution is negligible; on the other hand, average contributions of up to 7 % and 17 % are observed for Models 2 and 3, respectively. Even though it is not shown in the paper, it is important to mention that

contributions of up to 30 % are observed for some individual strong motions for the case of Model 3. Unlike axial loads, the contribution does not increase as one moves up the building. The contribution of the LR and VD modes for bending moments in beams was also calculated but the results are not presented. The contribution is, however, quite similar to that of bending moments in columns.

7.2. Contributions in terms of global response parameters

The contributions of the LR and VD modes, in terms of interstory shears and interstory displacements, as for the case of local parameters were also calculated for every story, model and structural direction. However, no graph is given only the main results are briefly presented. Similar to the case of bending moments, the contribution is negligible, moderate and significant for the 3-, 9-, and 20-storey models, respectively. The maximum contributions for interstory shears are 5 % and 19 % for the 9-, and 20-storey models, respectively. The corresponding contributions for interstory displacements are 6 % and 21 %.

8. Objective 3: Individual contribution of the LR and VD modes

In Section 7 of the paper, the simultaneous contribution of the LR and VD modes in terms of several response parameters was discussed.

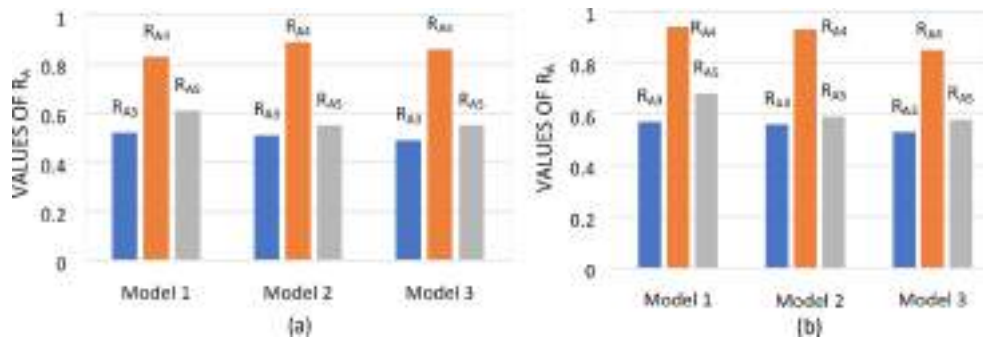


Fig. 10. Values of the R_{A3} , R_{A4} and R_{A5} ratios for the NS direction; (a) exterior columns, (b) interior columns.

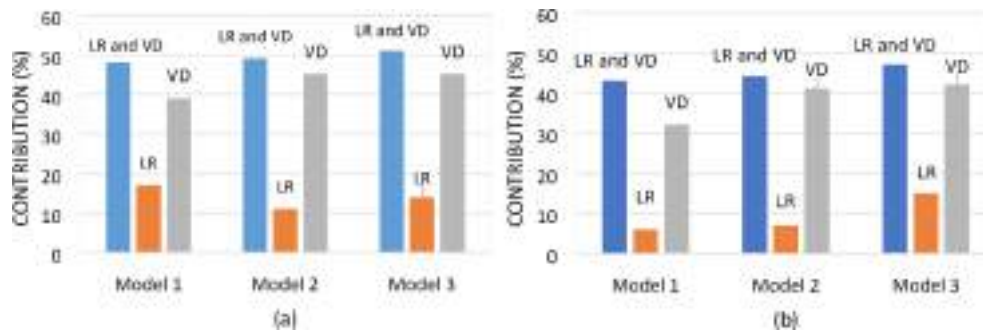


Fig. 11. Combined and individual contributions in terms of axial load of the LR and VD modes, NS direction;(a) exterior columns, (b) interior columns.

However, the following question remains: how is the contribution of the LR modes compared to that of the VD ones? This issue is addressed in this part of the paper. Only the contribution in terms of axial loads on columns is briefly presented since it was significant for all the models.

The individual contributions of the LR and VD modes are measured by the R_{A4} and R_{A5} ratios, which are mathematically expressed by Eqs. (16) and (17), respectively. In such equations, the term $A4(3,20,3)$ represents the axial load on columns obtained by considering $\zeta = 3\%$ in the LD and VD modes and $\zeta = 20\%$ in the LR ones. The term $A4(3,3,20)$ has a similar meaning but $\zeta = 3\%$ is used in the LD and LR modes, and $\zeta = 20\%$ in the VD modes. The other parameters in the equations were defined earlier.

$$R_{A4} = \frac{A4(3, 20, 3)}{A3(3, 3, 3)} \tag{16}$$

$$R_{A5} = \frac{A5(3, 3, 20)}{A3(3, 3, 3)} \tag{17}$$

Only the results for exterior and interior columns of the NS direction are given, the results for the EW direction are quite similar. The maximum mean values of the R_{A3} , R_{A4} and R_{A5} parameters, which corresponds to the maximum considered seismic intensity, can be seen in Fig. 10a and 10b for exterior and interior columns, respectively. The corresponding contributions (in percentage) are given in Fig. 11.

Results indicate that the individual contribution of the VD modes is, as expected, greater than that of the LR modes. However, the latter is not negligible. Taking into account the three models, the overall individual contributions of the LR and VD modes for the case of exterior columns are about 28% and 87%, respectively, of that of the combined modes. The corresponding percentages are about 20% and 86% for interior columns.

9. Conclusions

Seismic analysis of different structures, including those of steel buildings, is normally based on a damping matrix derived according to

the Rayleigh Model (C_R). It has been shown in the literature that many problems arise if this model is used. It is accepted that the damping matrix (C_S) derived from the superposition of modal damping matrices (SMDM) gives more accurate results. However, nothing has been stated regarding the contribution of the higher modes of vibration associated to local rotations (LR) and vertical displacements (VD). Illustrating a few of the inconveniences of using the C_R matrix as well as some issues related to the contribution of the LR and VD modes constitutes the main objective of this paper. Three steel moment-resisting frames of different heights, modeled as complex MDOF systems, and twenty strong motion records are used in the study. The main findings are:

1. The concept of effective modal mass (EMM) is used to define if the modes are of type LD, LR or VD. It is observed that the order of the modes can be mixed and that the LR and VD modes can be associated to significant amounts of EMM. For example, for the 9-storey model used in the study, the first five modes are LD type, but mode 6 is VD type, having an EMM of 48%.
2. If the SMDM procedure and only lateral displacements (LD) modes are used to form the damping matrix, in order to avoid amplification of the response, a certain percentage of damping should be given at least in the lower LR and VD modes.
3. The underestimation of axial loads on columns can be larger than 40% if the matrix C_R is used with respect to the result of the matrix C_S . The corresponding level of underestimation of bending moments on beams and columns can be larger than 30%.
4. The contribution of the LR and VD modes to axial loads and bending moments can be, on an average basis, larger than 50% and 17%, respectively. The contribution in terms of interstory shears and drifts is also significant; on average it can be larger than 20%.
5. The individual contribution of the VD modes in terms of axial loads is, as expected, greater than that of the LR modes. However, the latter is not negligible. Considering all three models, the overall individual contributions of the LR and VD modes are approximately 28% and 87%, respectively, of that of the combined modes.

6. In light of the findings of this study, it is strongly recommended to use the SMDM procedure to form the damping matrix and to consider the contributions of the LR and VD modes when calculating the seismic response.

The presented study was limited to plane frames that are regular in-plan and elevation. Other aspects like irregularity and 3D models need to be considered to get more general conclusions.

Declaration of Competing Interest

The authors declare that they have no known competing financial interests or personal relationships that could have appeared to influence the work reported in this paper.

Data availability

No data was used for the research described in the article.

Acknowledgments

This paper is based on work supported by El Consejo Nacional de Ciencia y Tecnología (CONACyT), México, under grant CB/2016-287103 and by the Universidad Autónoma de Sinaloa, under grant PRO_A8_013.

References

- Clough R, Penzien J. Dynamics of structures. 3rd ed. Berkeley, CA: Computers & Structures Inc.; 1995.
- Paz M, Leigh W. Structural dynamics – theory and computation. 5th ed. Boston, MA: Kluwer Academic Publishers; 2004.
- Chopra A. Dynamics of structures. New Jersey: Prentice Hall; 2012.
- Chopra AK, McKenna F. Modeling viscous damping in nonlinear response history analysis of buildings for earthquake excitation. Earthq Eng Struct Dyn 2016;45:193–211. <https://doi.org/10.1002/eqe.2622>.
- Rea D, Clough RW, Bouwkamp JG. Damping capacity of a model steel structure; 1971.
- Wilson EL, Penzien J. Evaluation of orthogonal damping matrices. Int J Numer Methods Eng 1972;4:5–10. <https://doi.org/10.1002/nme.1620040103>.
- Chrisp DJ. Damping models for inelastic structures. Christchurch: University of Canterbury; 1980.
- Léger P, Dussault S. Seismic-energy dissipation in MDOF structures. J Struct Eng 1992;118:1251–69. [https://doi.org/10.1061/\(ASCE\)0733-9445\(1992\)118:5\(1251\)](https://doi.org/10.1061/(ASCE)0733-9445(1992)118:5(1251)).
- Bernal D. Viscous damping in inelastic structural response. J Struct Eng 1994;120:1240–54. [https://doi.org/10.1061/\(ASCE\)0733-9445\(1994\)120:4\(1240\)](https://doi.org/10.1061/(ASCE)0733-9445(1994)120:4(1240)).
- Val DV, Segal F. Effect of damping model on pre-yielding earthquake response of structures. Eng Struct 2005;27:1968–80. <https://doi.org/10.1016/j.engstruct.2005.06.018>.
- Hall JF. Problems encountered from the use (or misuse) of Rayleigh damping. Earthq Eng Struct Dyn 2006;35:525–45. <https://doi.org/10.1002/eqe.541>.
- Li Y-H, Wu B. Determination of equivalent damping relationships for direct displacement-based seismic design method. Adv Struct Eng 2006;9:279–91. <https://doi.org/10.1260/136943306776986930>.
- Zareian F, Medina RA. A practical method for proper modeling of structural damping in inelastic plane structural systems. Comput Struct 2010;88:45–53. <https://doi.org/10.1016/j.compstruc.2009.08.001>.
- Rodríguez H, Varum H, Arède A, Costa A. A comparative analysis of energy dissipation and equivalent viscous damping of RC columns subjected to uniaxial and biaxial loading. Eng Struct 2012;35:149–64. <https://doi.org/10.1016/j.engstruct.2011.11.014>.
- Jehel P, Léger P, Ibrahimbegovic A. Initial versus tangent stiffness-based Rayleigh damping in inelastic time history seismic analyses. Earthq Eng Struct Dyn 2014;43:467–84. <https://doi.org/10.1002/eqe.2357>.
- Carr AJ, Puthanpurayil AM, Lavan O, Dhakal R. Damping models for inelastic time-history analyses—a proposed modelling approach. In: 16th World Conf Earthq; 2017.
- Kollár LP, Pap ZB. Modal mass of floors supported by beams. Structures 2018;13:119–30. <https://doi.org/10.1016/j.istruc.2017.12.002>.
- Gioncu V, Mazzolani F. Seismic design of steel structures. CRC Press; 2013. doi: 10.1201/b16053.
- Mazzolani F, Piluso V. Theory and design of seismic resistant steel frames. CRC Press; 2012. doi: 10.1201/9781482271348.
- Ferraioli M, Lavino A, Mandara A. Behaviour factor of code-designed steel moment-resisting frames. Int J Steel Struct 2014;14:243–54. <https://doi.org/10.1007/s13296-014-2005-1>.
- Elghazouli AY. Assessment of European seismic design procedures for steel framed structures. Bull Earthq Eng 2010;8:65–89. <https://doi.org/10.1007/s10518-009-9125-6>.
- Landolfo R. Seismic design of steel structures: new trends of research and updates of eurocode 8; 2018. p. 413–38. doi: 10.1007/978-3-319-75741-4_18.
- Zhang H, Zhu X, Li Z, Yao S. Displacement-dependent nonlinear damping model in steel buildings with bolted joints. Adv Struct Eng 2019;22:1049–61. <https://doi.org/10.1177/1369433218804321>.
- Zand H, Akbari J. Selection of viscous damping model for evaluation of seismic responses of buildings. KSCE J Civ Eng 2018;22:4414–21. <https://doi.org/10.1007/s12205-018-0860-6>.
- Milanchian R, Hosseini M. Study of vertical seismic isolation technique with nonlinear viscous dampers for lateral response reduction. J Build Eng 2019;23:144–54. <https://doi.org/10.1016/j.jobbe.2019.01.026>.
- Jafari M, Alipour A. Methodologies to mitigate wind-induced vibration of tall buildings: a state-of-the-art review. J Build Eng 2021;33:101582. <https://doi.org/10.1016/j.jobbe.2020.101582>.
- Qian X, Chopra AK, MF. Modeling viscous damping in nonlinear response history analysis of steel moment-frame buildings: design-plus ground motions. Berkeley; 2020.
- Sun F-F, Yang J-Q, Wang M, Wu T-Y. An adaptive viscous damping wall for seismic protection: experimental study and performance-based design. J Build Eng 2021;44:102645. <https://doi.org/10.1016/j.jobbe.2021.102645>.
- Clough RW. On the importance of higher modes of vibration in the earthquake response of a tall building*. Bull Seismol Soc Am 1955;45:289–301. <https://doi.org/10.1785/BSSA0450040289>.
- Maniatakis CA, Psycharis IN, Spyarakos CC. Effect of higher modes on the seismic response and design of moment-resisting RC frame structures. Eng Struct 2013;56:417–30. <https://doi.org/10.1016/j.engstruct.2013.05.021>.
- Qiu C-X, Zhu S. High-mode effects on seismic performance of multi-story self-centering braced steel frames. J Constr Steel Res 2016;119:133–43. <https://doi.org/10.1016/j.jcsr.2015.12.008>.
- Vafaei M, Alih SC. Influence of higher order modes and mass configuration on the quality of damage detection via DWT. Earthq Struct 2015;9:1221–32. [10.1298/9/eas.2015.9.6.1221](https://doi.org/10.1298/9/eas.2015.9.6.1221).
- Chen L, Tremblay R, Tirca L. Practical seismic design procedure for steel braced frames with segmental elastic spines. J Constr Steel Res 2019;153:395–415. <https://doi.org/10.1016/j.jcsr.2018.10.010>.
- Almitani KH, Abdelrahman AA, Eltaher MA. Influence of the perforation configuration on dynamic behaviors of multilayered beam structure. Structures 2020;28:1413–26. <https://doi.org/10.1016/j.istruc.2020.09.055>.
- Lu Y, Hao G, Han Q, Huang J. Steel tubular friction damper and vibration reduction effects of double-layer reticulated shells. J Constr Steel Res 2020;169:106019. <https://doi.org/10.1016/j.jcsr.2020.106019>.
- Rahmani AY, Bourahla N, Bento R, Badaoui M. Adaptive upper-bound pushover analysis for high-rise moment steel frames. Structures 2019;20:912–23. <https://doi.org/10.1016/j.istruc.2019.07.006>.
- Kinoshita T, Nakamura N, Kashima T. Characteristics of the first-mode vertical vibration of buildings based on earthquake observation records. JAPAN Archit Rev 2021;4:290–301. <https://doi.org/10.1002/2475-8876.12208>.
- Bhattacharjee T, Chanda D, Saha R. Influence of soil flexibility and plan asymmetry on seismic behaviour of soil-piled raft-structure system. Structures 2021;33:1775–88. <https://doi.org/10.1016/j.istruc.2021.05.045>.
- Gremer N, Adam C, Furtmüller T. Effect of damping model and inelastic deformation on the prediction of vertical seismic acceleration demand on steel frames. Bull Earthq Eng 2022. <https://doi.org/10.1007/s10518-022-01530-9>.
- Luco JE, Lanzani A. Numerical artifacts associated with Rayleigh and modal damping models of inelastic structures with massless coordinates. Earthq Eng Struct Dyn 2019;48:1491–507. <https://doi.org/10.1002/eqe.3210>.
- Luco JE, Lanzani A. A new inherent damping model for inelastic time-history analyses. Earthq Eng Struct Dyn 2017. <https://doi.org/10.1002/eqe.2886>.
- Cruz C, Miranda E. Evaluation of damping ratios for the seismic analysis of tall buildings. J Struct Eng 2017;143. [https://doi.org/10.1061/\(ASCE\)ST.1943-541X.0001628](https://doi.org/10.1061/(ASCE)ST.1943-541X.0001628).
- Bernal D, Döhler M, Kojidi SM, Kwan K, Liu Y. First mode damping ratios for buildings. Earthq Spectra 2015;31:367–81. <https://doi.org/10.1193/101812EQS311M>.
- Carr A. RUAUMOKO, Inelastic dynamic analysis program; 2016.
- Chen WF, Tsutsu T. Interaction equations for biaxially loaded sections. 1971.
- Krawinkler H. The state-of-the-art report on system performance of moment resisting steel frames subjected to earth quake ground shaking. Building 2000.
- Eads L, Miranda E, Lignos G. Seismic collapse risk assessment of buildings: effects of intensity measure selection and computational approach. Stanford, CA; 2014.
- Elkady A, Lignos DG. Effect of gravity framing on the overstrength and collapse capacity of steel frame buildings with perimeter special moment frames. Earthq Eng Struct Dyn 2015;44:1289–307. <https://doi.org/10.1002/eqe.2519>.